Title

Ultrastructure Expansion Microscopy (U-ExM) in *Trypanosoma cruzi*: localization of tubulin isoforms and isotypes

Author and Affiliation

Victoria Lucia Alonso[1,2]*

[1] Instituto de Biología Molecular y Celular de Rosario, CONICET. Rosario, Argentina.

[2] Facultad de Ciencias Bioquímicas y Farmacéuticas, Universidad Nacional de Rosario. Rosario, Argentina.

*Corresponding author

e-mail: alonso@ibr-conicet.gov.ar

Phone number: +54 0341 4350661 extension 133

Abstract

Ultrastructure Expansion Microscopy (U-ExM) is a recently developed technique that enables the increase of the spatial resolution within a cell or a tissue for microscopic imaging by physically expanding the sample. For the first time, I report a detailed protocol validating the use of U-ExM in *Trypanosoma cruzi* and quantifying the expansion factors of different subcellular compartments. I was able to determine the localization patterns of different tubulin isoforms, such as α-tubulin and β-tubulin. Also, I immunolocalized acetylated and tyrosinated α-tubulin isotypes in epimastigotes and use mitochondrial cell-permeable dyes to identify this organelle. Finally, U-ExM was also performed in trypomastigotes and amastigotes validating this technique in all life cycle stages of *T. cruzi*.

Keywords

Confocal microscopy, cytoskeleton, acetylation, tyrosination, mitochondria

29 **Introduction**

30 *Trypanosoma cruzi*, a kinetoplastid parasite and the etiological agent of Chagas disease or
31 American trypanosomiasis, has with a complex life cycle that alternates between a mammalian
32 and an insect host (Triatominidae family), which is the biological vector of this disease (Lidani
33 et al. 2019). The World Health Organization classifies Chagas disease as one of the 13 most
34 neglected tropical diseases, constituting a very important social and economic problem, especially
35 in Latin America.

36 Trypanosomatids are characterized by a precisely organized cytoskeletal constituted by stable
37 microtubules (MT), which is simpler in comparison with other eukaryotic cells. Such MTs are
38 present in the mitotic spindle, the basal body, the flagellar axoneme, and the subpellicular
39 microtubules. The latter are connected to each other and to the plasma membrane forming a
40 helical arrangement along the central axis of the parasite cell body (de Souza 2009). MTs are
41 composed by α/β-tubulin heterodimers forming helical tubes and provide the basis for
42 cytoskeletal architecture. They are regulated by interacting with a variety of MT-associated
43 proteins (MAPs), by a differential expression of α- and β-tubulin genes (tubulin isotypes), and by
44 tubulin isoforms generated by the inclusion of different post-translational modifications (PTMs)
45 in each isotype (Gadadhar et al. 2017). In trypanosomatids, many PTMs were identified across
46 the microtubular array. It is proposed that this could be used to control the differential recruitment
47 of MAPs and motors during the cell cycle (Sinclair and de Graffenried 2019).

48 Ultrastructure Expansion microscopy (U-ExM) has been introduced recently as a super-resolution
49 microscopy technique. Basically, biological specimens are included in swellable polymer
50 hydrogels and then are physically expanded to resolve fine details (Chen et al. 2015). This method
51 its very simple and accessible, its compatibility with conventional fluorescent probes, and
52 inexpensive chemicals. It can achieve a spatial resolution of ~65 nm using conventional
53 (confocal) microscopes, around four times better than the standard resolution of a confocal
54 microscope (~250 nm).

55 Since 2015 there has been a steady growth of the publication involving this technique, especially
56 in protozoan parasites, like *Giardia lamblia*, *Plasmodium falciparum,* and *Toxoplasma gondii*

57 (Tillberg and Chen 2019; dos Santos Pacheco and Soldati-Favre 2021; Gorilak et al. 2021;
58 Tomasina et al. 2021). This technique was first reported in the kinetoplastid *Trypanosoma brucei,*
59 where a component of the mitochondrial genome segregation machinery was described (Amodeo
60 et al. 2021; Kalichava and Ochsenreiter 2021), but it has not been reported in *T. cruzi*.
61 In this report, I validate the use of U-ExM in *Trypanosoma cruzi* and quantify the expansion
62 factors of different subcellular structures. I describe the localization patterns of tubulin isoforms,
63 such as α-tubulin, β-tubulin, validating this technique in all life cycle stages of *T. cruzi*. Also, I
64 immunolocalized acetylated and tyrosinated α-tubulin isotypes in epimastigotes to visualize
65 subpellicular microtubules, the flagellar axoneme, the basal body, and the flagellar pocket.
66 Furthermore, I validated the use of the cell-permeable dyes, such as Mitotracker, for U-ExM in
67 *T. cruzi*.

68 **Methods**

69 Parasite culture and infections

70 *T. cruzi* Dm28*c* epimastigotes and Vero cells (ATCC CCL-81) were cultured and infected as
71 previously described (Alonso et al. 2016).

72 U-ExM protocol

73 I started with 5 million epimastigotes or trypomastigotes, washed the pellets twice with 500 µl
74 PBS and centrifuged for 5 min at 2000 g, then resuspended in 200 µl of PBS and settled for 20
75 min at room temperature on poly-D-lysine coated coverslips (12 mm, Marlenfeld GmbH). For
76 mitochondrial staining, epimastigotes were resuspended in PBS and incubated with 1mM
77 Mitotracker Orange CMTMRos (Invitrogen) for 30 min at 28°C, washed twice in PBS and fixed
78 with 3% paraformaldehyde + 0.1% Glutaraldehyde (Sigma, 70% solution) in PBS for 15 min at
79 RT and then settled on coverslips as described before. Cells infected with amastigotes in 12 mm
80 coverslips were washed twice with PBS to eliminate culturing media. For all the conditions stated
81 above, coverslips were carefully submerged into a 24-well plate with 1 ml of 4% Formaldehyde
82 (FA, 36.5–38%, Sigma) and 4% acrylamide (AA, 40% stock solution, Invitrogen) in PBS and
83 incubated for four to five hours at 37°C. For gelation, coverslips were putted, with the cells facing

84 down, into 35µl of monomer solution: 19% Sodium Acrylate (Sigma), 10% AA, 0.1% N, N'-
85 methylenbisacrylamide (BIS, Sigma) in PBS, supplemented with 0.5% APS (Sigma) and 0.5%
86 tetramethylethylenediamine (TEMED, Sigma). A drop of monomer solution was placed over a
87 parafilm in a pre-cooled humid chamber for each coverslip. For gelation, samples were incubated
88 5 mins on ice, and then for 1 h at 37°C in the dark. Coverslips with gels were then transferred into
89 a six-well plate filled with 2 ml of denaturation buffer (200 mM sodium dodecyl sulfate (SDS),
90 200 mM NaCl, and 50 mM Tris-HCl in MilliQ, pH 9) for 15 min at room temperature with gentle
91 agitation to allow the gels to detach from the coverslips. Gels were then moved into a 1.5 ml
92 Eppendorf centrifuge tube filled with 1 ml denaturation buffer and incubated at 95°C for 1 h and
93 30 min. After denaturation, gels were placed in 50 ml beakers or Petri dishes filled with MilliQ
94 water for the first round of expansion. Water was exchanged after 30 minutes and then gels were
95 incubated overnight in MilliQ water. The next day, water was exchanged one more time for 30
96 minutes and then gels were washed two times for 30 min in PBS (to allow gel shrinkage) and
97 subsequently incubated with primary antibody (Table I), all antibodies were diluted in 2%
98 PBS/BSA, and gels were incubated for 3 h at 37°C and then overnight at 4ºC in 24 well plates
99 with 300 µl of the diluted antibodies. Gels were then washed in PBS-T three times for 10 min
100 while gently shaking and subsequently incubated with secondary antibodies (Table I) using the
101 same incubation times. The day after, gels were washed in PBS-T (three times for 10 min while
102 shaking) and placed into beakers or Petri dishes filled with MilliQ water for the second round of
103 expansion. Water was exchanged three times every 30 min. After this step, gels were carefully
104 measured with a caliper showing an expansion factor between 4.2x and 4.6x. The specificity of
105 the antibodies was verified by western blot with epimastigotes' total extracts (Figure 1a).

106 Imaging and measurement of the expansion

107 The gel was then cut with a razor blade into pieces and put into a 35 mm glass-bottom dish
108 (Matsunami) previously coated with poly-lysine for confocal imaging. Confocal microscopy was
109 performed on a Zeiss LSM880 using a 63x oil NA 1.4 objective, with the following parameters:
110 z step size at 0.65 µm interval with a pixel size of 0.132 nm. ZEN BLACK 2.1 SP3 software

111 (Zeiss, RRID:SCR_018163) and Fiji (Schindelin et al. 2012) (RRID:SCR_002285) were used to
112 analyze the images.
113 To determine the expansion factor, the ratio of expanded kinetoplast and nucleus to non-expanded
114 epimastigotes was calculated (n = 20 cells) using GraphPad Prism v. 9.0.1 (RRID:SCR_002798).
115 The length of the kinetoplast was determined by measuring its maximum length and the diameter
116 of the nucleus by measuring the widest diameter of each epimastigote using Fiji.

117 **Results and Discussion**

118 U-ExM workflow in *T. cruzi*

119 Although the Ex-M protocols present in the literature follow the same steps, they have differences
120 regarding the concentration of fixative agents, denaturing agents, and incubation times (this also
121 depends on the nature of the protein to be immunolocalized). I tested several conditions and
122 optimized the workflow for *T. cruzi* (Figure 1), which is described in Methods section. In this
123 report, I used antibodies against cytoskeletal proteins (insoluble proteins) (Table I) and gave a
124 detailed protocol to perform the U-ExM, but is important to mention that the incubation time
125 when targeting soluble proteins or membrane proteins the incubation time and temperature during
126 the denaturing step should be optimized.
127 As observed in Figure 1, in the first step, FA and AA (precursor molecules) are introduced to
128 functionalize the cellular components, this allows the subsequent linkage of swellable
129 polyelectrolyte gel (Monomer solution containing SA). The gel formation is accomplished using
130 the oxidizing reagents TEMED and APS (as for standard polyacrylamide gels). Then, the parasite
131 contents are denatured using SDS and high temperature. After this step, the first round of
132 expansion is performed in ultrapure water followed by incubation in PBS, where the gel shrinks
133 again. Finally, standard immunofluorescence techniques are applied followed by the second
134 round of expansion in water before imaging in an epifluorescence or confocal microscope.

135 Localization of tubulin isoforms

136 MTs are essential components of the eukaryotic cytoskeleton and cell division machinery. I
137 immunolocalized α- and β-tubulina using specific monoclonal antibodies (Figures 2a and 2b). A
138 similar localization pattern was observed for both isoforms at the subpellicular microtubules and

139 the flagellar axoneme. The axoneme is immunostained from the base of the flagellum to its tip,
140 in continuous attachment to the cell body as previously described (de Souza 2009)). Pro-and
141 mature basal bodies were also clearly observed, as well as the microtubule quartet in proximity
142 to the kinetoplast in a parasite that is starting to divide (Zoom in Figure 2b) (Elias et al. 2007).
143 Alpha-tubulin was also immunolocalized in trypomastigotes and amastigotes, highlighting this
144 technique's value in all life cycle stages of *T. cruzi*. As observed in figure 2c the subpellicular
145 array and the flagellar axoneme are clearly immunostained in both stages. It is interesting to note
146 that the anti α-tubulin antibody used (TAT-1), immunodetects, in our experimental conditions,
147 exclusively amastigotes' α-tubulin and not the host cell protein, I believe this is because TAT-1
148 was developed by immunizing mice with extracted *T. brucei brucei* cytoskeleton although it is
149 suitable to use in mammalian cells.

150 Localization of tubulin isotypes in *T. cruzi*

151 There are many conserved acetylated lysines (K) reported in α- and β-tubulin, but acetylation of
152 the α-tubulin luminal residue K40, discovered over thirty years ago, has been widely
153 characterized. This acetylation mark is associated with stable microtubes and with the resistant
154 microtubules to depolymerizing drugs (L'Hernault and Rosenbaum 1985). In Trypanosomatids
155 subpellicular, mitotic and axonemal microtubules are extensively acetylated making them
156 interesting models for studying K40 acetylation (Sasse and Gull 1988; Souto-Padron et al. 1993).
157 As observed in Figure 3, acetylated α-tubulin is presenten in the subpellicular microtubules and
158 flagellar axoneme. Immunodetection of the flagellar pocket (Figure 3a) and the basal body is also
159 observed in great detail using U-ExM. Tyrosinated α-tubulin shows a different localization
160 pattern (Figure 3b). The subpellicular MTs of the posterior end of the cell body, the nascent flagellum
161 of dividing cells, and the basal bodies are all immunodetected, similar to the localization reported for
162 *T. brucei* (Sherwin et al. 1987). A weak reaction is detected in the subpellicular MTs of the anterior
163 part of the epimastigotes and the old flagellum.

164 Measurement of subcellular compartments and structures in epimastigotes

165 Trypanosomatids are characterized by a single flagellum and a mass of mitochondrial DNA
166 organized into a kinetoplast connected to the proximal end of the basal bodies and the flagellar

167 pocket (Gull 1999). The kinetoplast was measured in epimastigotes stained with Mitotracker and
168 for nuclear measurements, I stained epimastigotes' DNA with DAPI (Figure 3c). With
169 Mitotracker staining, the ramifications of the single mitochondria of *T. cruzi* are clearly identified
170 and the kinetoplast is deeply marked, this also allowed us to validate the use of cell-permeable
171 dyes for U-ExM in *T. cruzi*. Using DAPI I was able to discriminate condensed regions of the
172 chromatin as well as the nucleolar domain (identified by the lack of DAPI staining) (Figure 3c).
173 An expansion factor of 4.2x and 4.6x was quantified for the nucleus and the kinetoplast
174 respectively, which signifies that expansion was homogeneous within the cells (Figure 3d).
175 When compared with non-expanded epimastigotes, the resolution gain is clear and allowed us to
176 visualize the potential of this technique in *T. cruzi* (Figure 3e). In conclusion, U-ExM is a
177 powerful approach for studying cytoskeletal structures in *T. cruzi*. It is a robust super-resolution
178 method, but it is very simple and does not need highly specialized reagents or instrumentation.
179 U-ExM allows high-resolution imaging, improving the axial and lateral effective resolution of the
180 molecules to be analyzed. An expansion factor of four increases resolution from around 250 nm
181 to less than 70 nm using regular confocal microscopy. In the future, this could be further improved
182 by super-resolution techniques to visualize biomolecular structures that are in close proximity to
183 each other, such as the components of the flagellar pocket and basal body, which are poorly
184 described in *T. cruzi*.

185 **Statements and Declarations**

186 Competing interest

187 The authors have no relevant financial or non-financial interests to disclose.

188 Funding

189 This work was supported by Agencia Nacional de Promoción Cientifica y Tecnológica from
190 Argentina (PICT2017-1978 and PICT2019-0526) and the Research Council United Kingdom
191 (MR/P027989/1).

192 Authors contribution statement.

193 VLA has designed, performed the experiments, and wrote the manuscript.

194 Acknowledgments.

Thanks to Dr. Esteban Serra and Dr. Luis E. Tavernelli for the critical reading of the manuscript. I am also very grateful to Rodrigo Vena for assisting in the acquisition of confocal images.

References

Alonso VL, Ritagliati C, Cribb P, et al (2016) Overexpression of bromodomain factor 3 in Trypanosoma cruzi (Tc BDF3) affects parasite differentiation and protects it against bromodomain inhibitors. FEBS Journal 283:2051–2066. https://doi.org/10.1111/febs.13719

Amodeo S, Kalichava A, Fradera-Sola A, et al (2021) Characterization of the novel mitochondrial genome segregation factor TAP110 in Trypanosoma brucei. Journal of Cell Science 134:. https://doi.org/10.1242/JCS.254300/237572

Chen F, Tillberg PW, Boyden ES (2015) Expansion Microscopy. Science (New York, NY) 347:543. https://doi.org/10.1126/SCIENCE.1260088

de Souza W (2009) Structural organization of Trypanosoma cruzi. Memórias do Instituto Oswaldo Cruz 104 Suppl:89–100

dos Santos Pacheco N, Soldati-Favre D (2021) Coupling Auxin-Inducible Degron System with Ultrastructure Expansion Microscopy to Accelerate the Discovery of Gene Function in Toxoplasma gondii. Methods in molecular biology (Clifton, NJ) 2369:121–137. https://doi.org/10.1007/978-1-0716-1681-9_8

Elias MC, da Cunha JPC, de Faria FP, et al (2007) Morphological Events during the Trypanosoma cruzi Cell Cycle. Protist 158:147–157. https://doi.org/10.1016/j.protis.2006.10.002

Gadadhar S, Bodakuntla S, Natarajan K, Janke C (2017) The tubulin code at a glance. Journal of Cell Science 130:1347–1353. https://doi.org/10.1242/jcs.199471

Gorilak P, Pružincová M, Vachova H, et al (2021) Expansion microscopy facilitates quantitative super-resolution studies of cytoskeletal structures in kinetoplastid parasites. Open Biology 11:. https://doi.org/10.1098/RSOB.210131

Gull K (1999) The cytoskeleton of trypanosomatid parasites. Annual review of microbiology 53:629–655

Kalichava A, Ochsenreiter T (2021) Ultrastructure expansion microscopy in Trypanosoma brucei. Open Biology 11:. https://doi.org/10.1098/RSOB.210132

223 L'Hernault SW, Rosenbaum JL (1985) Chlamydomonas .alpha.-tubulin is posttranslationally
224 modified by acetylation on the .epsilon.-amino group of a lysine. Biochemistry 24:473–478.
225 https://doi.org/10.1021/bi00323a034
226 Lidani KCF, Andrade FA, Bavia L, et al (2019) Chagas Disease: From Discovery to a Worldwide
227 Health Problem. Frontiers in Public Health 7:1–13.
228 https://doi.org/10.3389/fpubh.2019.00166
229 Sasse R, Gull K (1988) Tubulin post-translational modifications and the construction of
230 microtubular organelles in Trypanosoma brucei. Journal of Cell Science 90:577 LP – 589
231 Schindelin J, Arganda-Carreras I, Frise E, et al (2012) Fiji: an open-source platform for
232 biological-image analysis. Nature methods 9:676–682.
233 https://doi.org/10.1038/NMETH.2019
234 Sherwin T, Schneider A, Sasse R, et al (1987) Distinct localization and cell cycle dependence of
235 COOH terminally tyrosinated alpha-tubulin in the microtubules of Trypanosoma brucei
236 brucei. J Cell Biol 104:439–446
237 Sinclair AN, de Graffenried CL (2019) More than Microtubules: The Structure and Function of
238 the Subpellicular Array in Trypanosomatids. Trends in Parasitology 35:760–777
239 Souto-Padron, Narcisa LCES, De Sousa W (1993) Acetylated alpha-tubulin in Trypanosoma
240 cruzi: inmunocytochemical localization. 88:517–528
241 Tillberg PW, Chen F (2019) Expansion Microscopy: Scalable and Convenient Super-Resolution
242 Microscopy. https://doi.org/101146/annurev-cellbio-100818-125320 35:683–701.
243 https://doi.org/10.1146/ANNUREV-CELLBIO-100818-125320
244 Tomasina R, González FC, Francia ME, et al (2021) Structural and Functional Insights into the
245 Microtubule Organizing Centers of Toxoplasma gondii and Plasmodium spp.
246 Microorganisms 2021, Vol 9, Page 2503 9:2503.
247 https://doi.org/10.3390/MICROORGANISMS9122503
248

249 **Table I: List of antibodies used and working dilutions**

250 **Fig. 1 a)** Specificity of the anti- α-tubulin (49,8 kDa), β-tubulin (49.7 kDa), acetylated (Ac) α-
251 tubulin and tyrosinated (Tyr) α-tubulin antibodies were verified by western blot against total
252 epimastigotes extracts. 1 million parasites were blotted per lane, goat anti-mouse IgG conjugated
253 to HRP was used as the secondary antibody. **b)** U-ExM workflow in *T. cruzi*. Servier Medical Art
254 was used to create this figure (smart.servier.com)

255 **Fig. 2 Tubulin isotypes during *T. cruzi* cell stages a)** Epimastigotes stained with anti α-tubulin
256 antibodies (greyscale or magenta; Alexa 555) and DAPI (cyan; kDNA and nuclear DNA). In
257 Zoom images: bb, basal body; k, linetoplast; n, nucleus **b)** Epimastigotes stained with anti β-
258 tubulin antibodies (greyscale or magenta; Alexa 555) and DAPI (cyan; kDNA and nuclear DNA).
259 In Zoom images: bb, basal body; pro-bb, pro basal body; k, kinetoplast; n, nucleus, F, flagella **c)**
260 Trypomastogotes (T) and amastigotes (A) stained with anti α-tubulin antibodies (magenta; Alexa
261 555) and DAPI (cyan; kDNA and nuclear DNA).

262 **Fig. 3 Tubulin isoforms, mitochondrial staining and expansion measurments in**
263 **epimastigotes a)** Epimastigotes stained with anti Acetylated (Ac) α-tubulin antibodies (greyscale
264 or magenta; Alexa 555) and DAPI (cyan; kDNA and nuclear DNA). In Zoom images: bb, basal
265 body; F, flagella **b)** Epimastigotes stained with anti Tyrosonated (Tyr) a-tubulin antibodies
266 (greyscale or magenta; Alexa 555) and DAPI (cyan; kDNA and nuclear DNA). In Zoom images:
267 bb, basal body; F, flagella **c)** Epimastigotes stained with the cell-permeable dye Mitotracker and
268 DAPI. In Zoom images: k, kinetoplast; n, nucleus; nuc, nucleolus **d)** Nucleus and kinetoplast
269 measurements in expanded and non-expanded epimastigotes using Fiji. Expansion factor was
270 calculated as the ratio between non-expanded and expanded measurements **e)** Non-expanded and
271 expanded epimastigotes stained with anti α-tubulin (greyscale; Alexa 555).

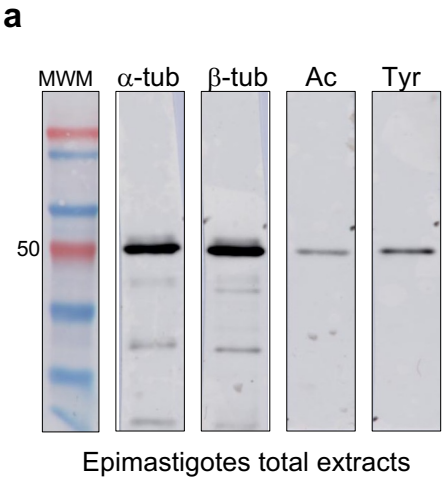
a
MWM
α-tub
β-tub
Ac
Tyr
50
Epimastigotes total extracts

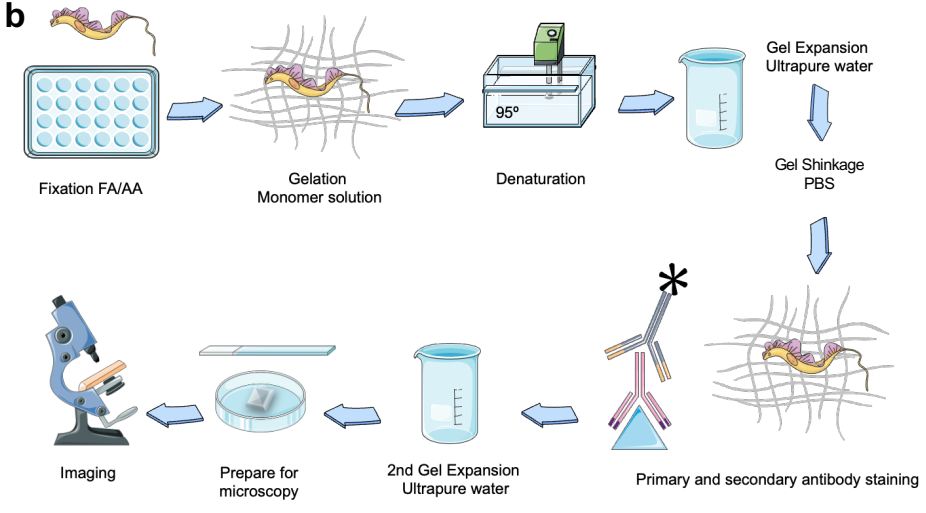
b
Fixation FA/AA
Gelation
Monomer solution
95º
Denaturation
Gel Expansion
Ultrapure water
Gel Shinkage
PBS
Primary and secondary antibody staining
2nd Gel Expansion
Ultrapure water
Prepare for
microscopy
Imaging

Fig 2

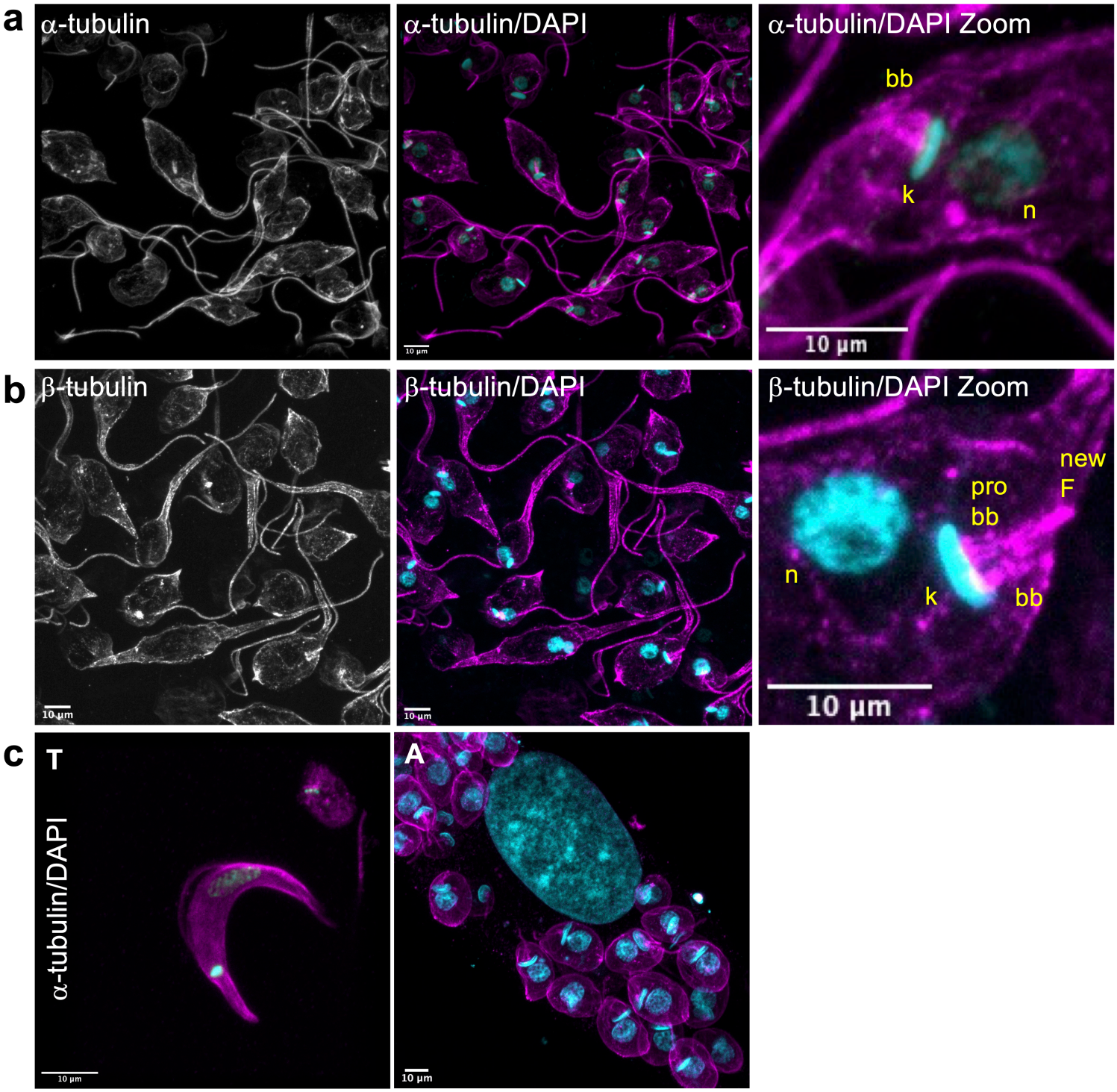
a
α-tubulin
α-tubulin/DAPI
α-tubulin/DAPI Zoom
bb
k
n
10 µm
b
β-tubulin
β-tubulin/DAPI
β-tubulin/DAPI Zoom
new
F
pro
bb
n
k
bb
10 µm
c
T
α-tubulin/DAPI
A
10 µm

Fig 3

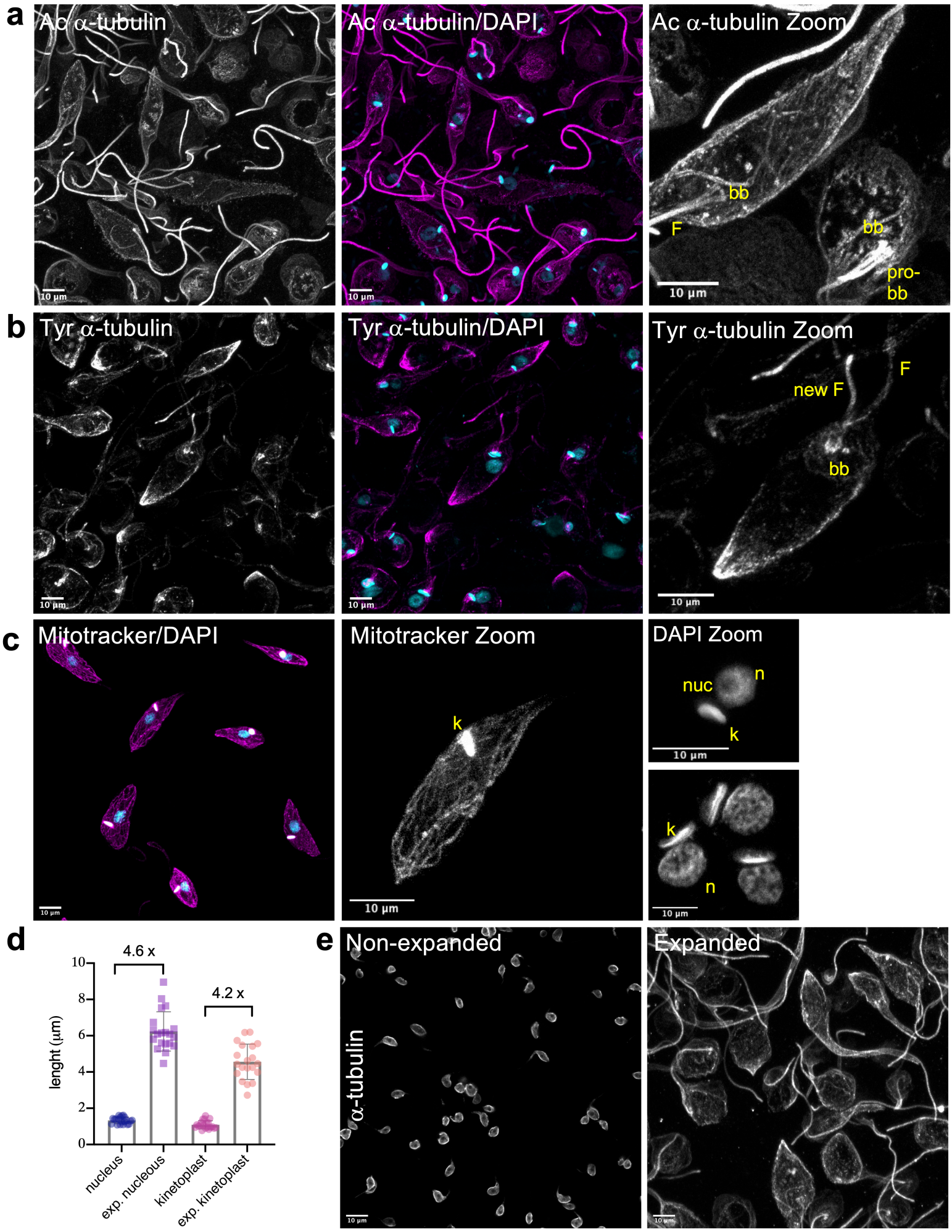
a
Ac α-tubulin
Ac α-tubulin/DAPI
Ac α-tubulin Zoom
bb
F
bb
pro-
bb
10 µm
b
Tyr α-tubulin
Tyr α-tubulin/DAPI
Tyr α-tubulin Zoom
F
new F
bb
c
Mitotracker/DAPI
Mitotracker Zoom
k
DAPI Zoom
nuc
n
k
d
4.6 x
4.2 x
lenght (µm)
nucleus
exp. nucleous
kinetoplast
exp. kinetoplast
e
Non-expanded
Expanded
α-tubulin